25

Receiver Front-End Architectures – Analysis and Evaluation

Pedro Cruz[#], Hugo Gomes[#*] & Nuno Carvalho[#]
[#]*Universidade de Aveiro (Instituto de Telecomunicações)*
Aveiro, Portugal
**Instituto Politécnico de Leiria (ESTG)*
Leiria, Portugal

1. Introduction

In today's world, the exponential growth from communications between people/companies in different places (at same time), the increasing requirement to measure and control all processes, the analysis in real time, the mandatory requirement to provide of information and entertainment data to electronic devices that must be increasingly smaller and more complex, requires a continuous and nonstop searching for new technologies with greater capacity, lower cost, reduced size and improved reliability.
The communications systems based on radio-frequency (RF) transmission are one of the greatest examples of this challenging demand. These systems, present in almost all equipment used in daily life as mobile phones, notebooks, wireless sensors, among other, require an increasing versatility and ability to storage of data, huge transmission rates of information and size reduction.
All this need for more sophisticated equipment, along with a greater number of services available in a single equipment (preferably portable), besides the drastic size reductions from the electronic components, requires a constant search for new architectures and new materials in order to maximize the features offered.
One of the most important parts from a RF system device is this receiver architecture. In receivers, the entry block has a key role in performance and reliability of the system. Any unresolved issue caused by this block, generates enormous problems in the following blocks of the receiver's architecture. For this reason, considering the constant increase of services available for the same frequency bands, associated with the growing number of users for each service, the entry receiver architecture must be capable to resolve issues such as blocking problems, peak-to-average power ratio (PAPR) problems, among others. In other hand, must be capable to offer good selectivity, sensitivity, lower energy consumption for a small price.
This chapter is organized in the following way. Firstly, a general review about the most common receiving architectures is done, emphasizing its main advantages and drawbacks. Moreover, some enhancements to these architectures are also presented and its principal benefits are explained, such as Hartley and Weaver configurations. This section ends with

some considerations about the implementation of adaptable wideband architectures and multi-standard operation. In the following section several interference problems as blocking and PAPR problems will be analyzed. Furthermore, a few techniques of PAPR reduction are overviewed to receiver application. After that, two possible application fields of these concepts are addressed, wherein two projects are shown regarding the radio-frequency identification (RFID) and software-defined radio (SDR) systems. Finally, the concluding remarks are drawn.

2. Review of Receiver Front-Ends Architectures

This chapter is intended to make a review of the main receiver's architectures known, show the main applications and study their main advantages and limitations (Besser & Gilmore, 2003), (Razavi, 1997), (Razavi, 1998).

2.1 Super-Heterodyne Receiver

The most common configuration used in RF receivers is the well known super-heterodyne architecture (Fig. 1). This configuration is based in two down-conversion stages, i.e., the RF received signal is first demodulated to an intermediate frequency (IF) and then converted to baseband signal. The received signal (Fig. 2a) is first filtered by a pre-selection filter and (after amplified by the low-noise amplifier, (LNA)) passes through another filter to reduce the image frequency effects before the first translation from RF to IF (Fig. 2b e 2c). After this stage, the signal is again filtered and demodulated to baseband (Fig. 2d), where it is converted to the digital domain where it can be processed. In this stage some architectures make an I/Q modulation in order to achieve better amplitude/phase information from the signal received.

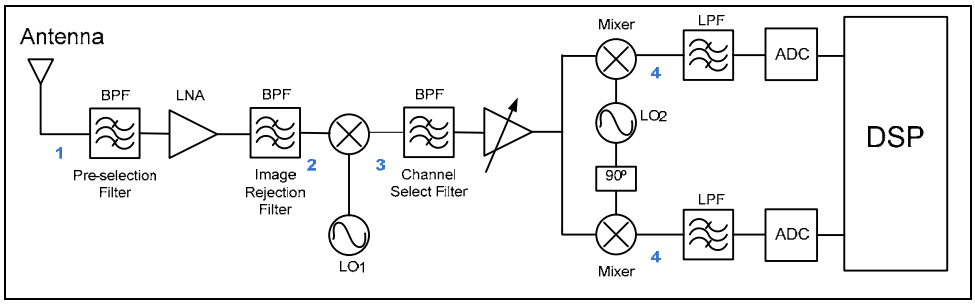

Fig. 1. A super-heterodyne receiver architecture

As referred above, this architecture is currently adopted in most radio receivers due to the availability of low-cost narrowband RF and IF components with low power consumption. Furthermore, this architecture can ensure good levels of sensitive (allows lower power signal at receiver input for which there is sufficient signal-to-noise ratio at the receiver output), selective (better ability to separate the desired band from signals received at other frequencies) and is immune to most DC problems affecting homodyne architecture.
However, super-heterodyne receivers have a number of substantial problems. The most important problem in this architecture is the cancellation from the image frequency. For a

good signal/image ratio is imperative that the image rejection filter has reduced transition band. To achieve this goal these filters must be performed by high-Q discrete components (SAW or ceramic filters), unpractical in today's IC technologies. For this reason, is not possible a full integration on-chip, resulting problems like perfect LNA 50 Ω load, noise figure and non-linear behaviour in discrete components. Another way to solve image frequency problem is the use of cancellation architectures such as Hartley or Weaver, presented in section 2.5.
Despite its greater complexity, the fact that it is designed for a specific channel (in a particular wireless standard) prevents the expansion of the receiving band.

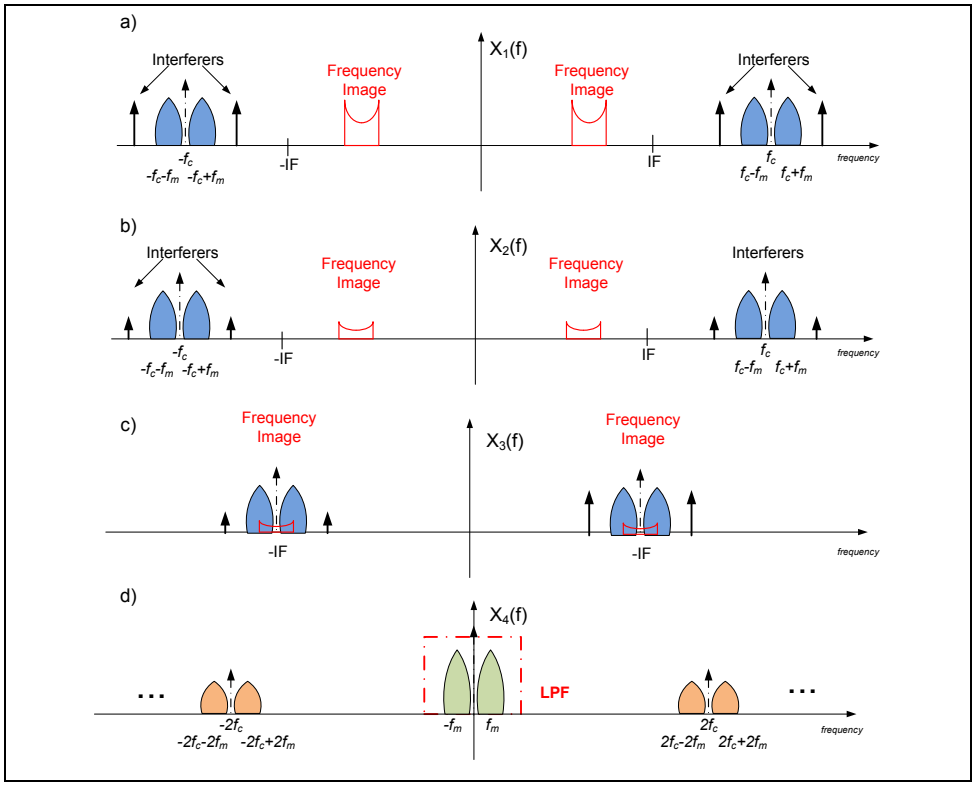

Fig. 2. Frequency domain operation of a super-heterodyne receiver

2.2 Zero-IF Receiver

Another typical receiver's architecture is the zero-IF receiver (Park et al., 2006), also known as homodyne receiver (Fig. 3). This architecture is a simplified version of the super-heterodyne, because instead of two down-conversion stages, it converts the RF signal directly to baseband. The received signal (Fig. 4a) is selected at RF by a band-pass filter, and then it is amplified by an LNA, as in the previous architecture (Fig. 4b). Finally, it is directly down converted to DC by a mixer (or two mixers with a delay of 90º between them) and converted to the digital domain using a straightforward analogue-to-digital converter

(ADC), (Fig. 4c). Compared to the last architecture this has a clear reduction in the number of analogue components and guarantees a high level of integration thanks to its simplicity.

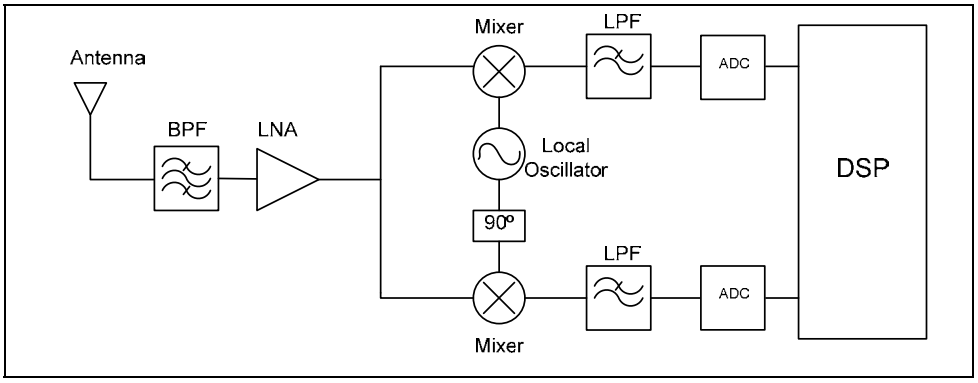

Fig. 3. A zero-IF receiver architecture

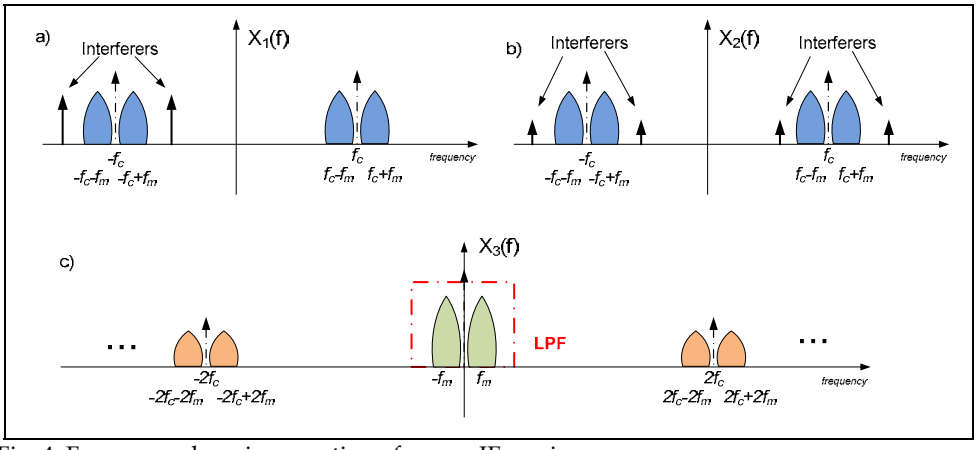

Fig. 4. Frequency domain operation of a zero-IF receiver

Despite its simplicity compared to the super-heterodyne architecture, many components of the zero-IF receiver are more complex to deploy. In addition the direct translation to DC can generate several problems that strongly conditioned the use of this architecture over the super-heterodyne. Problems as DC offset, such as local oscillator (LO) leakage due to non-ideal isolation between the port from the mixer or interferer leakage due to non-ideal isolation between the port from the mixer, I/Q mismatch due to errors in I/Q modulation, Even/Odd-order distortion caused by non-linear components generated several products in harmonic frequencies, specially second-order intermodulation products that are generated around DC and large flicker noise of the mixer can easily corrupt the output signal since it is a baseband signal. Some techniques to reduce these problems associated with the increasing integration of the constituent components of the zero-IF architecture has contributed to better performance and increased use.

2.3 Low-IF Receiver

A similar configuration to the previous one is the low-IF receiver (Adiseno et al., 2002), Fig. 5, in which the RF signal is mixed down to a nonzero low or moderate IF (few hundred kHz to several MHz) instead of going directly to DC, using quadrature RF down-conversion. This solution tries to combine the advantages from the zero-IF receiver and the super-heterodyne receiver. Like zero-IF receiver, the received signal (Fig. 6a) passes through a channel-selection filter at RF and is amplified by a LNA (Fig 6b). After this similar step, the signal is down converted to a low IF, instead of zero IF (Fig. 6c), and used an image suppression block in order to cancel the negative effects from frequency image. Finally, an ADC converts the signal to digital domain, allowing the use of digital signal processing algorithms. In some low-IF architectures the image suppression block is transferred to the digital domain.

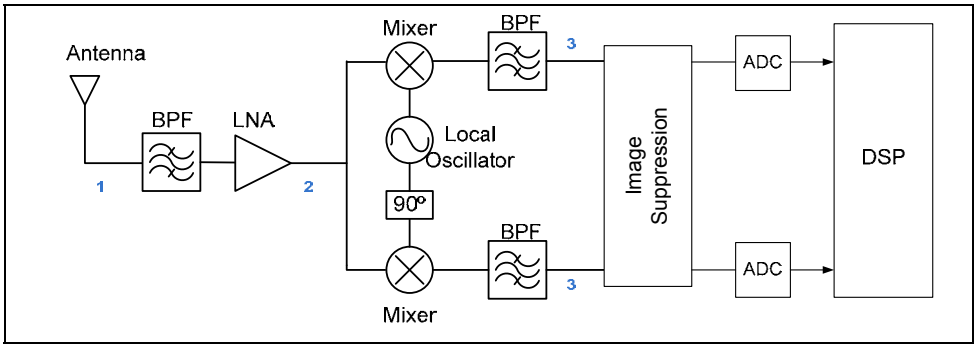

Fig. 5. A low-IF receiver architecture

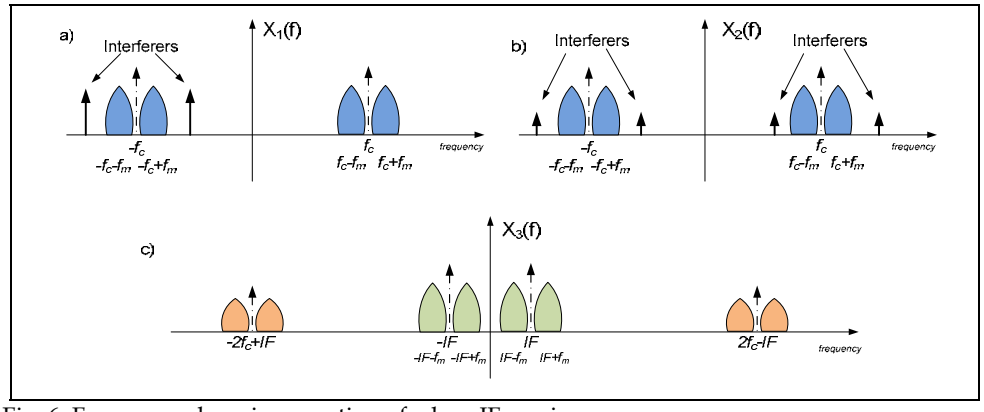

Fig. 6. Frequency domain operation of a low-IF receiver

This architecture still allows a high level of integration (advantage from zero-IF) but does not suffer from the DC problems (advantage from super-heterodyne), since the desired signal is not situated around DC. However, this architecture continued to suffer from the image frequency and I/Q mismatch problems (with greater impact than in previous

architectures) and the ADC power consumption is increased since now a high conversion rate is required.

2.4 Band-Pass Sampling Receiver

An alternative to the previous configurations is the band-pass sampling receiver (Vaughan et al., 1991), (Akos et al., 1999), Fig. 7. In this architecture, the received signal is filtered by an RF band-pass filter that can be a tuneable filter or a bank of filters, and then it is amplified using a wideband LNA. The signal is then converted to the digital domain by a high sampling rate ADC and digitally processed. All the previous architectures use analogue circuitry to down-convert the incoming RF signal to I and Q baseband components, and obtaining good matching in analogue circuits is not easy. In that sense, this architecture considers firstly an analogue to digital conversion and then the I/Q demodulation in the digital domain. In this way the I/Q matching is an all digital task and obtaining sufficient matching accuracy in two digital signal paths is easily accomplished. One means to generate these digitally I/Q signals is to use the Hilbert transform (Tsui, 1995). Thus, as in the low-IF architecture, here we can take advantage of digital signal processing to alleviate some issues of the analogue front-end. Moreover, pushing the analogue-to-digital conversion closer to the antenna provides an increased flexibility.

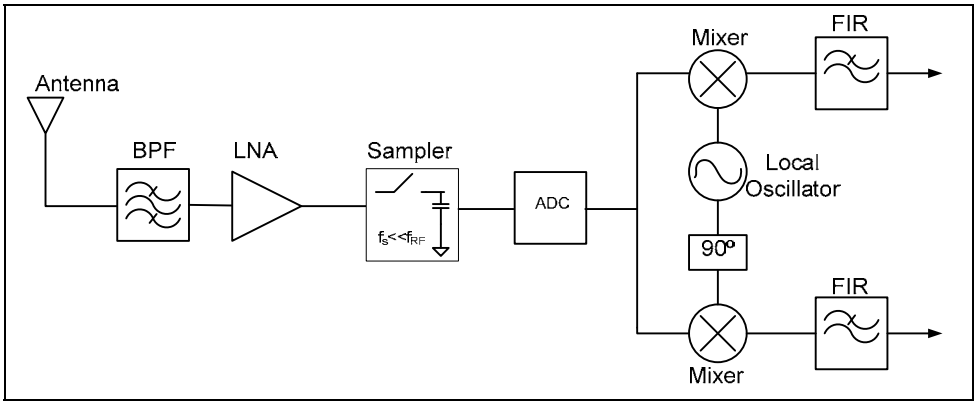

Fig. 7. A band-pass sampling receiver architecture

This configuration is based on the fact that all energy from DC to the input analogue bandwidth of the ADC will be folded back to the first Nyquist zone [0, $f_S/2$] without any mixing down conversion needed because a sampling circuit is replacing the mixer module. In Fig. 8, is shown the frequency domain operation of the band-pass sampling receiver. Whether a correct sampling frequency is chosen, it is possible to receive more than one RF signal at same time and then make its processing in the digital domain. Nevertheless, it is mandatory to include RF band-pass filtering in order to avoid overlap of other undesirable signals.

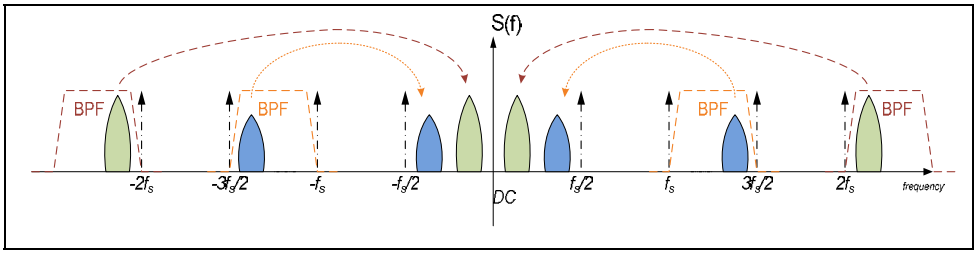

Fig. 8. Frequency domain operation of a band-pass sampling receiver

As was described in (Akos et al., 1999), it is possible to pinpoint the resulting intermediate frequencies, f_{IF}, based on the following relationship

$$if \quad fix\left(\frac{f_C}{f_S/2}\right) \quad is \quad \begin{cases} even, & f_{IF} = rem(f_C, f_S) \\ odd, & f_{IF} = f_S - rem(f_C, f_S) \end{cases} \tag{1}$$

where f_C is the carrier frequency, f_S is the sampling frequency, *fix(a)* is the truncated portion of argument *a*, and *rem*(*a*,*b*) is the remainder after division of *a* by *b*.
In this case, the RF band-pass signal filtering plays an important role because it must reduce all signal energy (essentially noise) outside the Nyquist zone of the desired frequency band that otherwise would be aliased. If not filtered, the signal energy (noise) outside the desired Nyquist zone is folded back to the first zone together with the desired signal, producing a degradation of the signal-to-noise ratio (SNR). This may be given by

$$SNR = 10.\log_{10}\left(\frac{S}{N_i + (n-1).N_0}\right) \tag{2}$$

where S represents the desired-signal power, N_i and N_0 are in-band and out-of-band noise, respectively, and n is the number of aliased Nyquist zones.
The advantage of this configuration is the sampling frequency needed and the subsequent processing rate are proportional to the information bandwidth, rather than to the carrier frequency. This reduces the number of components required. However, some critical requirements exist. For example, the analogue input bandwidth of the sample and hold circuit inside the ADC must include the RF carrier, which is a serious problem, considering the sampling rate of modern ADCs. Clock jitter can also be a vital problem when high frequencies implementations are considered.

2.5 Other Feasible Architectures

In addition to the main receiver architectures presented, there are other architectures / sub-architectures that are currently used or being developed. Some of these architectures are adaptations from older configurations that have been rearranged and use to very small circuits. As an example, the simple detector receiver (or envelope detector), used in the first AM radios, was reused for the development of very small tags (with very small

consumption) on RFID systems or even as power meters. Other architectures are use as support solutions to the previous receiver architectures problems, such as Hartley and Weaver configurations.

This section thus seeks to make a brief presentation of these architectures and a general review of all the architectures presented main advantages and limitations.

The envelope detector configuration (Fig. 9) is the most simple receiver architecture used because does not need of problematic components like mixers and local oscillators and the topology is very simple and cheap. The down-conversion method used in this architecture is based in the strong nonlinear behaviour from the diode. An interesting property of nonlinear systems is the spectral regrowth capability, which means that the system has the capability of create frequency components in the output signal that do not exist at the input side. As a result of this propriety, the received signal will present at diode output several replicas from the original signal in the harmonics and baseband frequencies. With the help of a low pass filter it is possible to eliminate all undesired frequencies and achieve the down-conversion of the desired signal without the use of mixers and local oscillators.

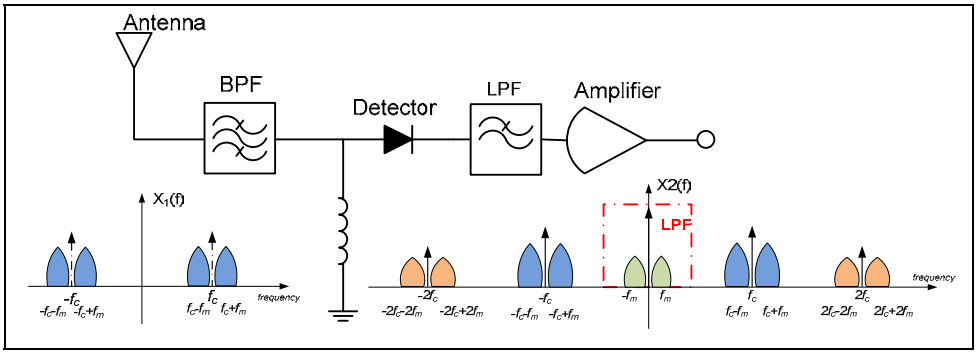

Fig. 9. Envelope detector configuration and frequency domain operation

This architecture is very useful in systems that require an extremely low energy consume such as passive RFID tags. The mains disadvantages of this receiver are the extreme intolerance to interferences, some DC problems (as zero-IF receiver) and very low sensitivity and selectivity, among others.

As was referred above, the Hartley and Weaver configurations are sub-architectures specially tailored to reduce/cancel the problems with the frequency image that affects strongly the super-heterodyne receiver. These architectures are similar but in last year's Weaver architecture have gained an advantage over the Hartley architecture, especially because of their better performance when integrated into IC.

The Hartley architecture (Fig. 10) uses an I/Q modulation in first stage and, after the low-pass filter, make a 90º time shift (Hartley shift) to invert the negative part from the spectrum. The sum of components I and Q results in the cancellation of the image frequency, and also strengthen the desired signal. The main advantages from this architecture are good image rejection ratio (IRR) and the immunity to load problems that results from the needless of high quality discrete components (needed in super-heterodyne). Although this configuration is very sensible to I/Q mismatch and the non-linear behaviour from the shift-by-90º and adder blocks can be extremely deteriorative for the output signal. The 90º shift

block is also difficult to realize and its behaviour is severely affected by the variation of the discrete components used in its design.

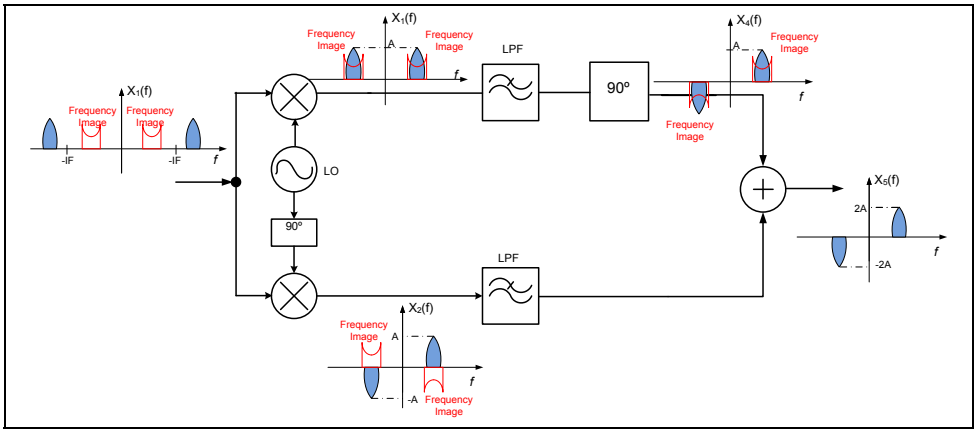

Fig. 10. Hartley image rejection configuration and frequency domain operation

The Weaver architecture is similar to Harley in first stage. Although, the shift-by-90º block is replaced by a second I/Q modulation. The two resulting signals can be subtracted and achieve the desired signal (with cancelation from the frequency image).

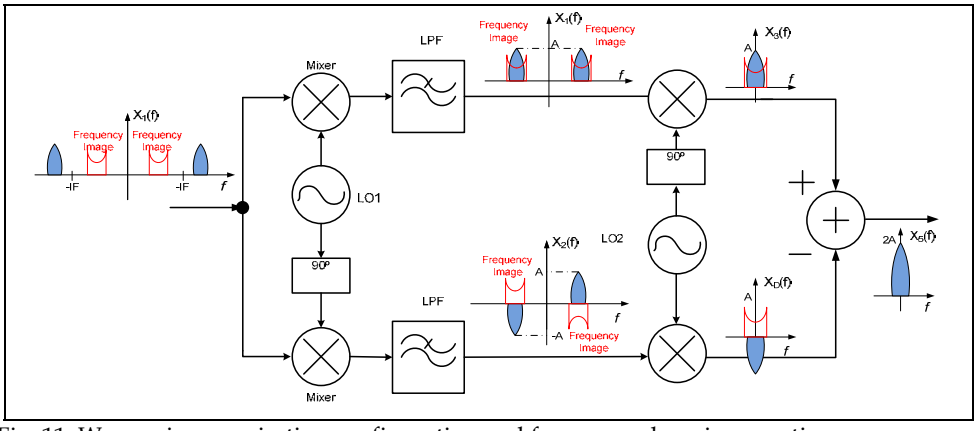

Fig. 11. Weaver image rejection configuration and frequency domain operation

The Weaver arrange has the advantage that do not depend from a difficult and no reliability shift-by-90º block and bring some flexibility to architecture because with a simple switch from the adder it is possible to achieve the desired signal or frequency image signal. With a most certain digitalization from several part from the receiver architectures, this configuration can ensure better results in technologies such as SDR. Nevertheless, the Weaver architecture has some limitations. Firstly, suffer the same I/Q mismatch problem as Hartley. Secondly, the huge number of mixers and LO amounts the energy consumption

and the cost of the topology. Finally, the temperature and process variation can significantly degrade the desired signal.
As a conclusion from the previous study of receiver architectures, in Table 1 are summarized the main advantages and major problems for each architecture.

Architecture	**Advantages**	**Major Problems**
Super-Heterodyne	- Selectivity - Sensitivity - Immune DC problems	- Image frequency - I/Q mismatch - High quality discrete components - Perfect LNA 50Ω load - Complexity - Noise figure - Nonlinear behaviour in components
Zero-IF	- Simplicity - IC integration	- Strong DC problems - I/Q mismatch - Even/Odd distortion - Flicker noise
Low-IF	- No DC problems - Simplicity - Less high quality discrete components	- I/Q mismatch - Image frequency - Requires high performance ADC
Band-Pass Sampling	- Flexibility - Signal manipulation - Low cost, circuit area - Minimize DC problems and RF problems (in digital domain)	- Susceptibility to clock aperture jitter - Noise figure degradation - Aperture distortion - Power consumption
Simple Detector	- Simplicity - Low cost	- Huge degradation with interferes - Low selectivity, sensitivity - Some DC problems
Hartley	- Good IRR - Less discrete components - Reduce load problems	- I/Q mismatch - Shift-by-90^{o} block and adder - Variation of R and C in RC-CR network - Increased number of components
Weaver	- Similar to Hartley - Avoid RC-CR network	- Huge number of mixers - I/Q mismatch - Dependent VCO - Strong adjacent channel interferes - Increased number of components

Table 1. Comparison of previous receiver architectures

Other architectures being proposed for use in the actual and future receivers involve use of direct RF sampling techniques based on discrete-time analogue signal processing to receive the signal, such as the ones developed in (Staszewski et al., 2004), (Muhammad et al., 2005). These methods are still in a very immature stage but should be further studied due to their potential efficiency in implementing reconfigurable receivers.

2.6 Path to Future Receivers

The holy grail of future RF architectures is that they will be able to receive any type of signal despite its bandwidth and dynamic range. Even though it is considered a holy grail, the path is moving towards multi-norm, multi-standard radios that are supported in SDR, and thus on that are capable of receiving a huge range of bandwidth combined with very different power levels, and thus dynamic range approaches.

This radios will move fast to be all digital, and completely defined by software. But, in order to achieve these master goals, much research and innovation still be needed. For instance in the receiving unit, the radio should have a very wide bandwidth ADC for gather and convert all the signals from analogue to digital, and this ADC should have a strong dynamic range associated, since it should receive low power signals combined with high power ones, and considering that if the radio has to receive several different signals, they should not combine each other.

In the transmitter side, the path is moving fast to the all digital PA, where the output signal is mainly a PWM modulated waveform that will traverse a switching amplifier, allowing an almost 100% efficiency, and the focus will be put on the output filter that will convert the digital waveform to analogue one, prior to feed the antenna.

Of course the last proposals are far from being possible, but researchers are moving toward there slowly.

3. Sources of Interference

In this section, we will give a detailed explanation about the complex problem related to interference between the strong transmitted signal and the weak received signal desired. This phenomenon is known as blocking. Moreover, we will analyze the impact of the signal peak-to-average power ratio, PAPR, in the receiving architectures. Another important point to be evaluated is the complexity increase that comes from the multi-standard implementation of the addressed receiving architectures. Both of these problems will provoke a limitation in the receiver's dynamic range. Moreover, some PAPR reduction techniques that can be applied in the receiver side will be described.

3.1 Blocking Problem

The co-existence of various technologies in the wireless spectrum has always led to problems of interference between systems. The regulatory authorities (whether national or international) try to avoid those interferences with rules and restrictions to RF systems that coexist in the same frequency band or adjacent frequency bands. However, even following all these standards and specifications, the presence of interference in a particular system is unavoidable, usually leading to degradation (or loss) of its quality and functionality. The dynamic range of a receiver front-end can be defined as the ratio between the maximum tolerable signal to the minimum detectable signal. This fact advises us that a receiver must be able to detect the weak desired signal and also have sufficient dynamic range to not be blocked by an undesired strong signal.

Thus, considering any of the previous presented architectures, the first nonlinear component that appears in the receiving chain is the LNA. This component is always nonlinear, since for a certain input the output signal is no longer proportional, neither follows the super-position principle (Pedro & Carvalho, 2003).

So, if we assume that a certain system wants to receive a signal with a desired power of, for instance, -70 dBm but another system that is adjacent to this one is emitting an interfering signal with a power of about 50 dBm, we can clearly conclude that if any intermodulation products arise in the receiver chain it will completely corrupt the desired signal.
In order to better understand this problem we will consider the previous cited example and analyze that in a detailed way. Therefore, the two signals are received and the interference signal will be attenuated by the receiver input filter, for which we have attributed an out-of-band rejection of around 50 dB. Although, a cascade of filters can be used to increase the out-of band attenuation, it will degrade the noise figure and also increase the insertion loss. That way, the interfering signal will be attenuated by around 50 dB and arrive to the input of the LNA with a power of 0 dBm. In Fig. 12 we can see a possible frequency domain representation of this situation.

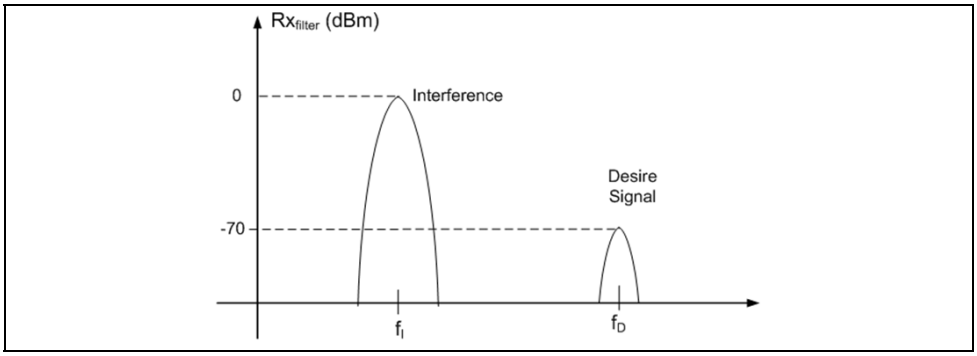

Fig. 12. Frequency domain schematic of the addressed interference situation

Thus, to study the possible intermodulation products in the example shown we will assume that the LNA is characterized by the following transfer function:

$$y_{LNA}(t) = a_1 x_{LNA}(t) + a_2 {x_{LNA}}^2(t) + a_3 {x_{LNA}}^3(t) \tag{3}$$

where x_{LNA} is the signal at the input port of the LNA, y_{LNA} is the output signal of the LNA, and a_1, a_2, and a_3 are model products coefficients.
Then, supposing that these two signals are two simple sinusoids, expression (4), we came up with a huge number of components in the outside of the LNA.

$$x_{LNA}(t) = A_1 \cos(w_1 t + \phi_1) + A_2 \cos(w_2 t + \phi_2) \tag{4}$$

where A_1 and A_2 are the amplitude components of interference and desire signal, and w_1 and w_2 are the respective frequency values.
Fig. 13 shows a complete overview of the frequency domain signal that is generated in the output of the LNA. If we look carefully to the third-order behaviour, we see that it will have a mixing product that falls exactly in the same frequency (w_2) of the desire signal. While the second-order and some of third-order intermodulation products can be eliminated by a filter that follows the LNA, there are the in-band third-order intermodulation products that

cannot be filtered out. Because we are assuming a very strong interference, A_1 is much higher than A_2, even if the LNA had very small intermodulation products (very low a_3), the interfering signal will continue to strongly affect the signal reception. As a result, development of techniques and sub-systems able to cancel, or at least mitigate, these adverse effects on radio receivers is of extreme importance.

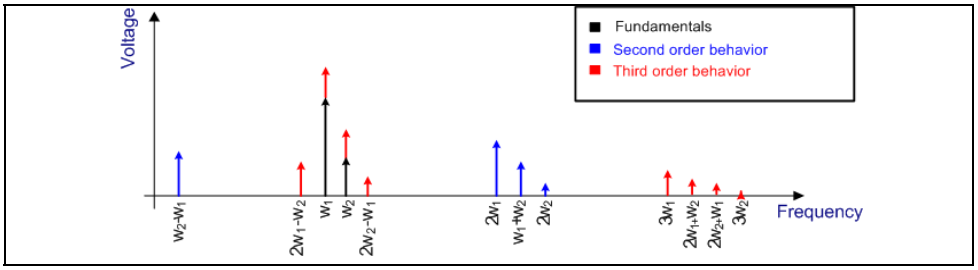

Fig. 13. Frequency domain schematic of the LNA output signal

3.2 PAPR Problem

PAPR is known since several years until now, actually the first known reference to this problem was made in (Landon, 1936), when he was studying the noise characteristics. The concept of PAPR is the relationship between the maximum value of the peak power and the average power of a given signal, and is a measure of great interest in actual wireless communications signals. It can be used for RF signal evaluation as well as for baseband signal evaluation (Bauml et al., 1996). Normally, this figure of merit is given in decibels and is calculated by using equation (5), where NT represents the number of samples considered for the PAPR evaluation.

$$PAPR_{dB} = 10.\log_{10}\left(\frac{\max\limits_{0\le t\le NT}|x(t)|^2}{mean\limits_{0\le t\le NT}|x(t)|^2}\right) \tag{5}$$

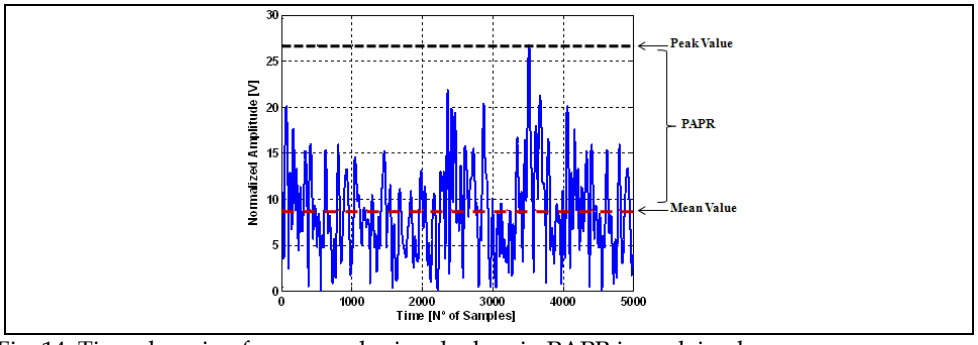

Fig. 14. Time-domain of an example signal wherein PAPR is explained

The previous figure shows an explanation of the PAPR calculation for a given example signal. There we can observe that a number of 5000 samples were used to determine the respective peak and mean values and in that way provide an estimate of the PAPR value.
The evaluation of the impact of PAPR in the communication systems components is mainly made through the analysis of complementary cumulative distribution function (CCDF) curves (Agilent App. Note, 2000), in which we define a certain percentage in the CCDF curve to pinpoint the reached PAPR value. The CCDF curves are closely related to the probability density function (PDF) of the signal because they are obtained by means of CCDF = 1 – CDF, where CDF is the cumulative distribution function that is obtained directly from the PDF statistics, as shown in equation (6):

$$cdf(x) = \int_{-\infty}^{a} pdf(x)dx \tag{6}$$

These curves provide a statistical description of the power levels in the signal and show how much time the signal spends at or above a certain power level. In the y-axis is represented the percent of time the signal power is at or above the power specified by the x-axis. An example of a CCDF curve is given in Fig. 15 using the previous presented signal. Analyzing the figure it is possible to affirm that the signal power exceeds the average by around 6 dB for 1% of the time (dashed red line) and also reach almost 8 dB for 0.01% of the time (dashed-point green line).

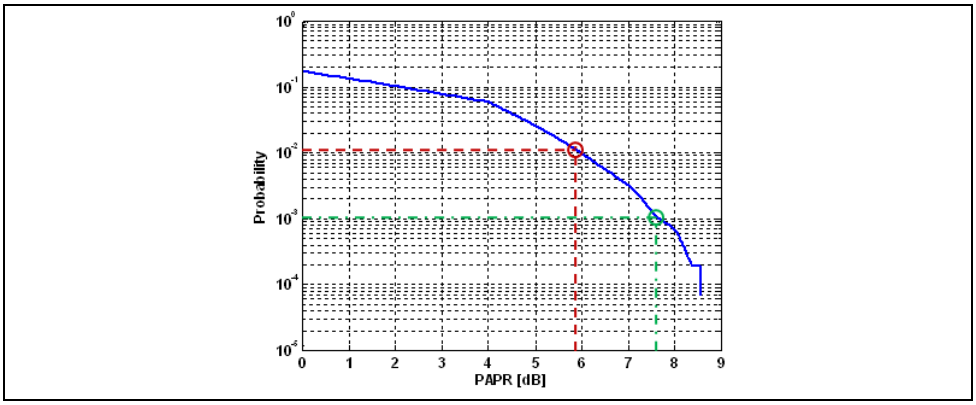

Fig. 15. CCDF curve for the previous presented example signal

Moreover, in actual wireless communications solutions, such as WiMAX (Worldwide Interoperability for Microwave Access) or 3GPP-LTE (Long Term Evolution), the receiving stages should deal simultaneously with a significant number of different signals due to the fact that they use an adaptive coded modulation algorithm (Goldsmith & Chua, 1998), which selects the best digital modulation format to apply based in a specific condition, for instance, SNR value. These digital modulation formats could vary from simple modulations as binary phase-shift keying (BPSK) to more complex formats as 64-QAM (quadrature amplitude modulation). Looking at Fig. 16, we can detect that these different modulation

formats will produce signals with slightly different PAPR values. This fact will impose different restrictions to the receiving components projected.

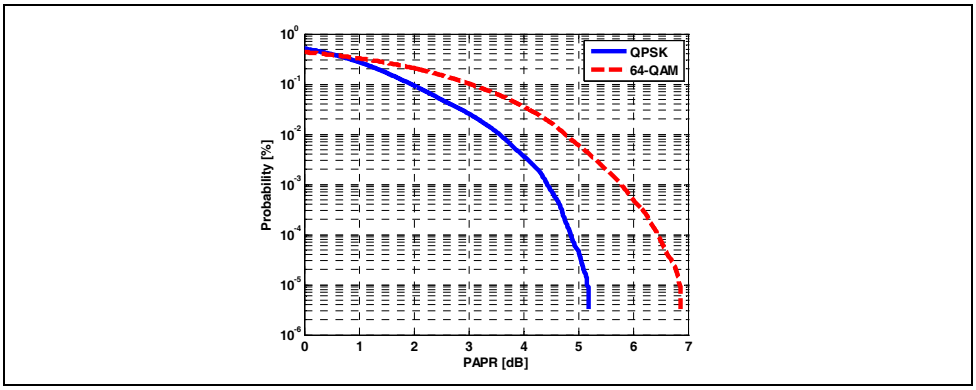

Fig. 16. CCDF curves for different signal modulation formats

Thus, it is mandatory to develop receiver configurations that can be capable to deal with the highest PAPR signal in order to not incite distortion generation. Adding to that fact, most of today standards has adopted the orthogonal frequency division multiplexing (OFDM) due to its spectral efficiency and capability to transmit high data rates over broadband radio channels. The main disadvantage of this technique is that it exhibits a high PAPR, which can be up to N times the average power (where N is the number of carriers).
So, the conjugation of both digital vector modulation formats and OFDM based schemes will lead to high values of PAPR, which limits the power that can be received or transmitted without distortion. This could lead to a necessity of using circuits with linear characteristics within a large dynamic range, otherwise the signal clipping at high levels would yield a distortion of the received signal. In fact, this PAPR problem immediately degrades the quality of the received signal because it will impose a degradation of the signal-noise ratio, SNR, in receiver ADC's accordingly to (7). If we allow the clipping of the signals peaks, then immediately the nonlinear distortion raises (Cruz et al., 2008).

$$SNR_{dB} = 6.02N + 1.76 - \alpha + 10.\log_{10}(2.OSR) \tag{7}$$

where N is the number of bits, a the PAPR and OSR the over-sample ratio.
One possible solution to this problem is to use crest factor minimization techniques (addressed in the following section), but in that case a care should be taken in order not to degrade either the nonlinear distortion, neither the error vector magnitude of the received symbols.
At the same time, a much more complex problem appears when we take into account the multi-carrier and multi-standard receiver or transmitter operation. Regarding the multi-carrier receiver operation, for instance, GSM (Global System for Mobile Communications) and W-CDMA (Wideband-Code Division Multiple Access) use a large number of channels and if we try to receive several channels at same time using a wideband receiver we will suffer from a problem created by the high PAPR of this multi-channel signal. In Fig. 17 is

shown the value of PAPR of a GSM signal using one and three channels, where the complexity of the three GSM channels significantly degrades the overall signal PAPR.

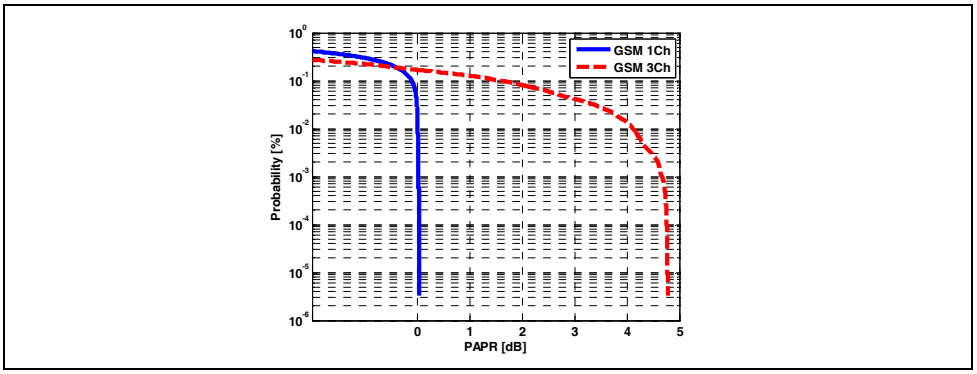

Fig. 17. CCDF curves for a 1-channel and 3-channels GSM signals

Concerning now on the multi-standard receiver operation we can also state that the PAPR of the multi-mode signals is always much higher than the single-mode configuration, as was demonstrated in (Cruz & Carvalho, 2008). Thus, in order to assess the complexity that we will be dealing with several combinations of usually used wireless standards were produced (using an arbitrary waveform generator), such as Wi-Fi and WiMAX (since they both work at near 2.4/2.5 GHz) and GSM-1800 with W-CDMA. In Table 2 are presented the relevant characteristics of the generated signals.

Signal Type	Frequency	Bandwidth	Multiplexing	Modulation
IEEE 802.11g	2.45 GHz	22 MHz	OFDM	64-QAM
IEEE 802.16e	2.502 GHz	14 MHz	OFDM	64-QAM
W-CDMA	1.9 GHz	3.84 MHz	-	π/4-QPSK
GSM-1800	1.81 GHz	200 kHz	-	GMSK

Table 2. Characteristics of the generated signals

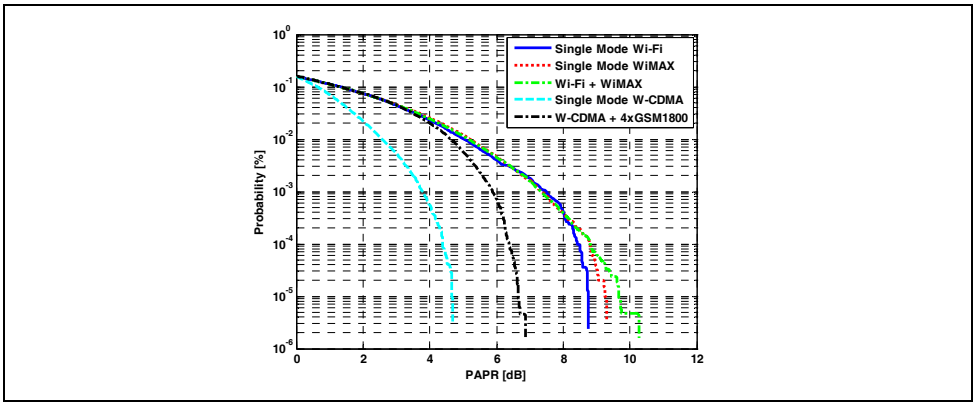

Fig. 18. CCDF curves for different multi-standard signal configurations

Fig. 18 shows the respective CCDF curves of each signal configuration (alone or in multi-mode operation) and it can be viewed that the multi-mode signals will produce more restrictions in terms of PAPR to the receiver components.

3.3 PAPR Reduction – *Required Techniques*

As was mentioned in the previous section with the constant development of the wireless world there will be need to solve or to minimize the problems that have been referred. Since several years ago the notion of PAPR reduction is being an important topic of researching in the scientific area. The increase in PAPR in multi-carrier systems becomes so complex that all the possible schemes for its minimization have become a goal for wireless system design engineers.

The approaches for that minimization spans from special coding for PAPR minimization (Han & Lee, 2005), tone reservation (Tellado & Cioffi, 1998), tone injection (Han et al., 2006), clipping followed by filtering (Vaananen et al., 2002), change of the constellation diagram (Krongold & Jones, 2003), and others based on representation of the signals to transmit (Han & Lee, 2003), like partial transmit sequences (PTS) interleaving or selected mapping (SLM).

Recently, the study has been centred not on how to minimize the PAPR exclusively, but on how to have a balance, on the minimum PAPR, transmission-rate and bit-error-rate (BER) optimization. We will focus our analysis in the techniques that can be used in the receiver for PAPR minimization instead of general techniques for PAPR reduction.

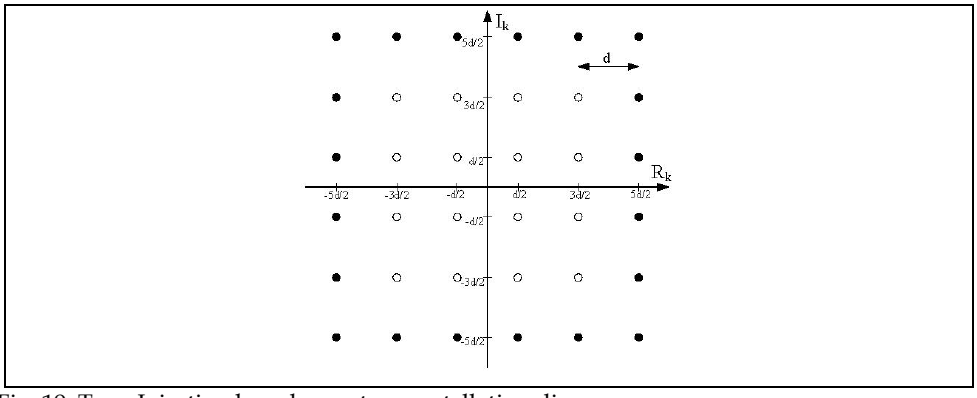

Fig. 19. Tone Injection based on extra constellation diagrams

Firstly, we have the Tone Injection technique (Han et al., 2006), in which the main idea is to create several constellation diagrams that can be dynamically chosen in order to reduce the PAPR. In fact, the addition of new constellation points in the constellation diagram is equivalent of injecting new tones. This new constellation point in the augmented constellation could be selected as to maintain the time waveform at a stable PAPR.

The idea from an OFDM point of view is nothing more than to add constants C to the OFDM symbol, which are carefully selected to reduce the PAPR and to not increase the BER. The effect of the added constant is to increase the constellation magnitude so that each of the point in the original constellation is mapped into the expanded constellation.

The values of C are $C_k = p_k D + jq_k D$, where p_k and q_k are chosen to minimize the PAPR value, and the constant D is known both at the transmitter and the receiver. Fig. 19 presents this solution for the case of a 16-QAM signal.
In Fig. 19, what we can see is that the black points could also be transmitted, but no new information is added. This means that we can transmit the same digital symbol either using the white points or the black points for the same base information bit, so the modulator have some redundancy, which is chosen in order to minimize the PAPR.
The main problem is the increase in BER. Nevertheless, the augmented capability to reduce PAPR is quite satisfactory.
Other possible available technique is the Tone Reservation (Tellado & Cioffi, 1998), where the underneath idea is to reserve, that means, to select some sub carriers in order that the overall RF signal has a reduced PAPR. In DSL communication systems this is normally done in the low SNR tones, since they will not be very important for the overall signal demodulation. So, in this case, we will add some information, C, to the unused tones to reduce the overall PAPR in the time domain scenario. The unused tones are called the reserved tones and normally do not carry data or they cannot carry data reliably due to their low SNR. It is exactly these tones that are used to send optimum vector C that was selected to reduce large peak power samples of OFDM symbols. The method is very simple to implement, and the receiver could ignore the symbols carried on the unused tones, without any complex demodulation process, neither extra tail bits.
Other simple but important technique is known as Amplitude Clipping plus Filtering (Vaananen et al., 2002), which is obviously the one that can achieve improved results and is less complex to apply. Nevertheless the clipping increases the occupied bandwidth and simultaneously degrades significantly the in-band distortion, giving rise to the increase of BER, due to its nonlinearity nature. The technique is based mainly on the following procedure: if the signal is below a certain threshold, then we let the signal as is, at the output, nevertheless if it passes that threshold then the signal should be clipped as is presented in expression (8).

$$y = \begin{cases} x & |x| \le A \\ Ae^{j\phi(x)}, & |x| \ge A \end{cases} \tag{8}$$

where $\phi(x)$ is the phase of the input signal x.
The main problem of this technique is that somehow we are distorting the signal generating nonlinear distortion both in-band and out-of-band. The in-band distortion cannot be filtered out, and some form of linearizer should be used or other form of reconstruction of the signal prior to the reception block. The out-of-band emission, usually called spectral regrowth, can be filtered out, but the filtering process will increase again the PAPR. For that reason, some algorithms are used sequentially with clipping and filtering in order to converge to a minimum value. This technique can be further associated with other schemes to improve the PAPR overall solution.
Finally, we describe a scheme that is called Companding / Expanding technique (Jiang et al., 2005), which is very similar to clipping, but the signal is not actually clipped, but rather companded or expanded accordingly to its amplitude. This technique was used since the

analogue telephone lines were the voice was companded in order to reduce its dynamic range problems encountered through the transmission over the copper lines. Most of the authors have dedicated their time to select the optimum form of the companding function in order to simultaneously reduce the PAPR and improve the BER performance. Fig. 20 presents one of these schemes implementation.

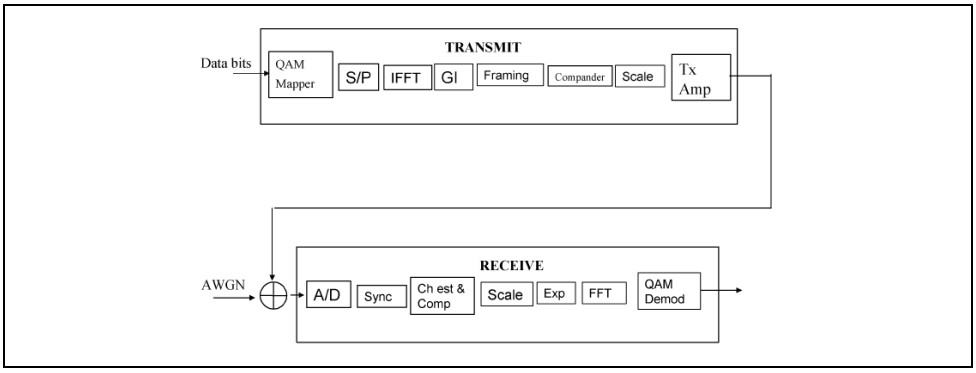

Fig. 20. Companding and Expanding implementation

One possibility for the companding function is the well-known μ-law, expression (9).

$$F(x) = \mathrm{sgn}(x)\frac{\ln\left(1+u|x|\right)}{\ln\left(1+u\right)}, \quad -1 \le x \le 1 \tag{9}$$

The drawbacks of this solution are similar to the clipping technique, but in this case the nonlinear distortion can be somehow post-distorted at the receiver more efficiently, since the nonlinearity is not as severe as the clipping form.

4. Example Applications

In this section, we will present possible real-world applications of several of previous described receiving architectures, in which we will describe some evaluated experiments. These include configurations that are being used in emergent fields, such as RFID and SDR systems. In these fields the multi-standard reception and the receiver PAPR minimization techniques analyzed can bring attractive improvements.

4.1 Radio Frequency Identification Applications

An RFID system is basically composed of two main blocks: the TAG and the READER (Fig. 21).

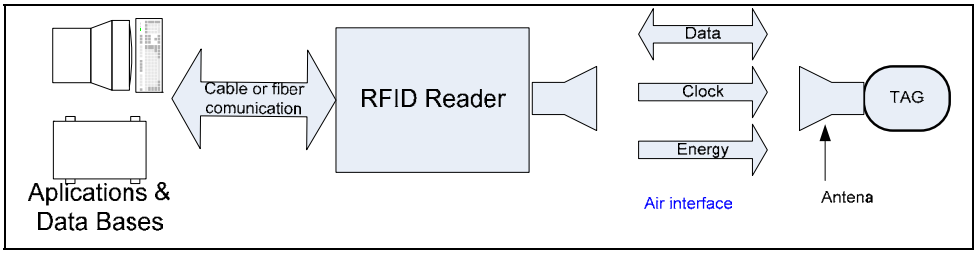

Fig. 21. RFID system

The Tag (or transponder) is a small device that serves as identifier of a person or an object in which it was implemented. When asked by the reader, returns the information contained within its small microchip. It should be noted, however, that despite this being the most common method, there are active tags that transmit information without the presence of the reader. The reader can be considered the "brain" of an RFID system. It is responsible for liaison between external systems of data processing (computer-data based) and the tags, it is also their responsibility to manage the system.

There are typically three main groups of tags: the passive, semi-passive (or semi-active) and active ones. These names derive from the needing of an internal battery for Tag's operation and transmission of signal. From these three types of Tags which will be addressed here is the semi-passive, to have a configuration very similar to the envelope detector architecture presented above. The spectral regrowth capability from the nonlinear behaviour of the diode is used in this topology, but instead of using the second harmonic product in baseband (like an envelope detector) it will use the third harmonic products (intermodulation products) that fall close to the original signal. The operational principle of the proposed approach is depicted in Fig. 22.

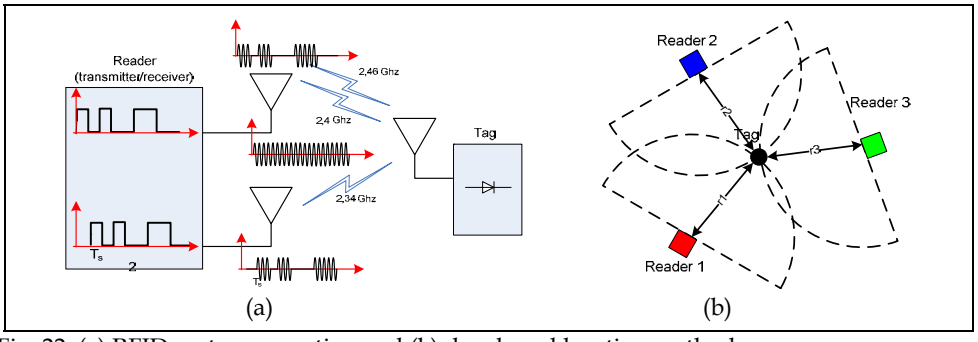

Fig. 22. (a) RFID system operation and (b) developed location method

The operational principle is as follows:

- The READER send an RF signal, at ω_2, modulated by a pseudo-random sequence and in a different frequency, ω_1, an un-modulated carrier RF signal.
- When the signal arrives to the TAG, a RF transceiver demodulates it and re-modulated in a different carrier and re-emitted to the air interface.

- The READER has a receiver tuned to this frequency, which allows to receive a replica of the transmitted signal.
- Now the two pseudo-random signals, the transmitted one, and the received one, could be compared in time, and the time of travel is calculated.
- This time delay indicates the distance between the READER and the TAG. Obviously, this distance is the ray of semi-circle with centre in the READER. For a correct location of the TAG, at least three different READERs are needed, as shown in Fig. 22(b).

This is a very simple procedure to locate the RFID. The use of an simple diode to generate a third harmonic product that can be used to re-emitted the signal back to the reader, prevents the process of demodulation and subsequent modulation of the data, do not need for local oscillators and reduce the number of a mixer, resulting a huge savings in energy consumption and cost of the components involved.
As seen, the only energy required in the Tag is the strictly necessary for the polarization of the diode. The entire RF path (reception and re-transmission) only use the energy of the signal received from the reader. In addition, this architecture enables the operation in full-duplex system, because the reader sends and receives on different frequencies allowing the simultaneous emission and reception.

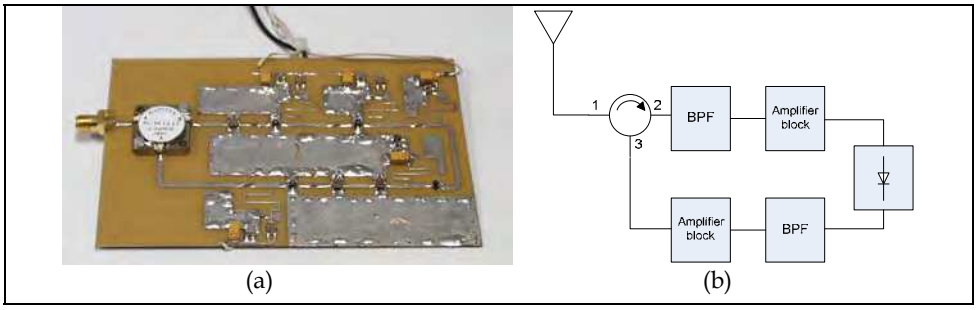

Fig. 23. (a) RFID Tag prototype and (b) block diagram

In Fig. 23 is presented the prototype of this simple envelope detector modified to this particularly case and its block diagram. The simple architecture and the small number of components could enable the full integration, creating an almost passive tag that would allow a location in real-time in full-duplex mode.
A more detailed description and some simulated and laboratory results can be found in any of these references (Gomes & Carvalho, 2007), (Gomes & Carvalho, 2008).

4.2 Software Defined Radio Applications

In order to demonstrate the application of the previous overviewed receiver architectures in SDR field, we have implemented, as an example, a band-pass sampling receiver, Fig. 7, using laboratory instruments. We used a fixed band-pass filter to select the fifth Nyquist zone to avoid aliasing of other undesired signals. This was followed by a commercially available wideband (0.5 – 1000 MHz) LNA with a 1 dB compression point of +9 dBm, an approximate gain of 24 dB, and a noise figure of nearly 6 dB. We used a commercially available 12-bit pipeline ADC that has a linear input range of approximately +11 dBm with an analogue input bandwidth of 750 MHz. Due to some limitations of the arbitrary

waveform generator used for the clock signal, a clock frequency of 100 MHz was utilized. The input RF frequency was in the fifth Nyquist zone, more precisely at f_{RF} = 220 MHz. In that sense, considering the clock frequency referred and the sample and hold circuit (inside the ADC) behaviour this RF signal was folded back to the first Nyquist zone, and fell in an intermediate frequency of f_{IF} = 20 MHz, obtained with equation (1). The feature of sub-sampling operation of the ADC, depicted in Fig. 8, was discussed in (Cruz et al., 2008) wherein the authors clearly demonstrate an ADC operating in a sub-sampled configuration obtaining very similar results in all of the Nyquist zones evaluated. Furthermore, in order to obtain accurate measurement results we used the set-up proposed in (Cruz et al., 2008a) shown in Fig. 24, to completely characterize our receiver, mainly in terms of nonlinear distortion.

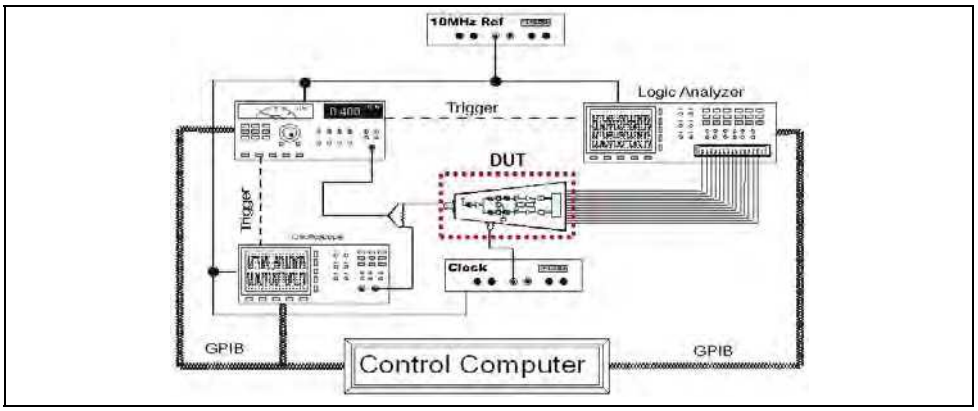

Fig. 24. Measurement set-up used in the characterization of the SDR front-end receiver

As can be seen from this set-up, the input signal was acquired by a sampling oscilloscope, while the output signal was acquired by a logic analyzer. The measured data were then post-processed using a commercial mathematical software package in the control computer. Then, we carried out measurements when several multisines having 100 tones with a total occupied bandwidth of 1 MHz were applied. We produced different amplitude/phase arrangements for the frequency components of each multisine waveform. In fact, these signals were intended to mimic different time-domain-signal statistics and thus provide different PAPR values (Remley, 2003), (Pedro & Carvalho, 2005). A WiMAX (IEEE 802.16e standard, 2005) signal was also used as the SDR front-end excitation. In this case, we used a single-user WiMAX signal in frequency division duplex (FDD) mode with a bandwidth of 3 MHz and a modulation type of 64-QAM (¾).

Fig. 25 presents the measured statistics for each excitation (multisines and WiMAX). The *Constant Phase* multisine is the one where the relative phase difference is 0º between the tones, yielding a large value of 20 dB PAPR. On the other hand, the uniform and normal multisines have uniformly and normally distributed amplitude/phase arrangements, respectively. These constructions yield around 2 dB PAPR for the uniform case and around 9 dB PAPR for the normal case. As can be observed in Fig. 25 the WiMAX signal is similar to the multisine with normal statistics.

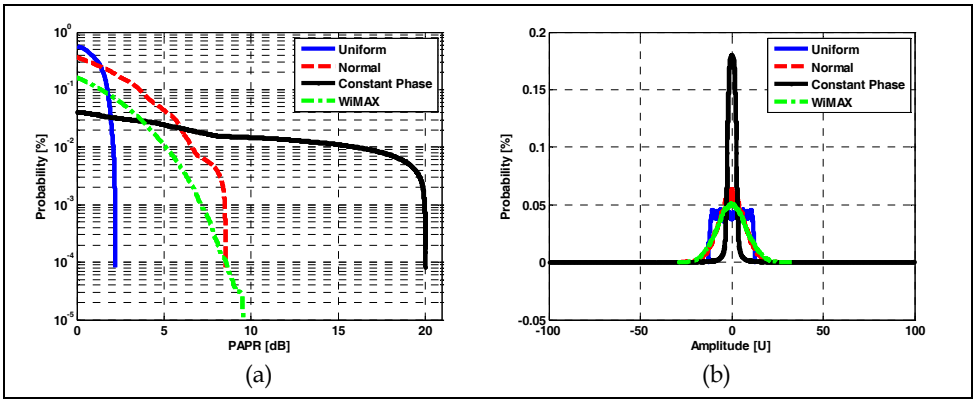

Fig. 25. Measured statistics for each excitation used, (a) CCDF and (b) PDF

Fig. 26 presents the measured results at the output of the SDR receiver using the logic analyzer, where the left graph shows the total power averaged over the excitation band of frequencies, while the right graph shows the total power in the upper adjacent channel arising from nonlinear distortion.

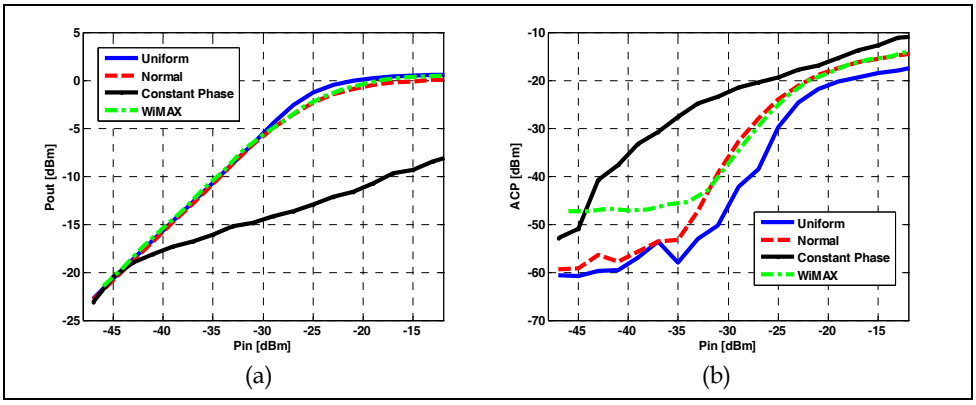

Fig. 26. Measured results at output of SDR receiver, (a) fundamental power and (b) adjacent channel power

It is clear that the signal with constant-phase statistics deviates from linearity at a much lower input power level than for the other cases since the PAPR of that signal is much higher and so clipping occurs at a relatively low input level. As well, the adjacent channel power is significantly higher for the constant phase case than for the others. As expected, the WiMAX signal performs very similarly to the multisine with normal statistics, both in the fundamental output power and in the adjacent channel power for a medium/large-signal operation (after around -30 dBm in its input). This happens because both signals have similar statistical behaviours. The higher small-signal adjacent channel power observed in the WiMAX signal compared to the multisine measurements is due to the intrinsic characteristics of this signal that is based on an OFDM technique, which results in a

significantly higher out-of-channel power. The obtained results allow us to stress that the signal PAPR could completely degrade the overall performance of such type of receiver in terms of nonlinear distortion and thus being a very important parameter in the design of a receiver front-end for SDR operation. Another point that is an open problem and should be evaluated is the characterization of SDR components, which is only possible with the utilization of a mixed-mode instrument as the one implemented in (Cruz et al., 2008a).

5. Summary and Conclusions

In this chapter we have presented a review of the mostly known receiver architectures, wherein the main advantages and relevant disadvantages of each configuration were identified. We also have analyzed several possible enhancements to the receiver architectures presented, which include Hartley and Weaver configurations, as well as new receiver architectures based in discrete-time analogue circuits.

Moreover, the main interference issues that receiver front-end architectures could experience were shown and analyzed in depth. Furthermore, some PAPR reduction techniques that may be applied in these receiver front-ends were also shown. In the final section, two interesting applications of the described theme were presented.

As was said, the development of such multi-norm, multi-standard radios is one of the most important points in the actual scientific area. Also, this fact is very important to the telecommunications industry that is expecting for such a thing. Actually, this is what is being searched for in the SDR field where the motivation is to construct a wideband adaptable radio front-end, in which not only the high flexibility to adapt the front end to simultaneously operate with any modulation, channel bandwidth, or carrier frequency, but also the possible cost savings that using a system based exclusively on digital technology could yield. It is expected that this chapter becomes a good start for RF engineers that wants to learn something about receivers and its impairments.

6. Selected Bibliography

Adiseno; Ismail, M. & Olsson, H. (2002). A Wideband RF Front-End for Multiband Multistandard High-Linearity Low-IF Wireless Receivers, *IEEE Journal of Solid-State Circuits*, Vol. 37, No. 9, September 2002, pp. 1162-1168, ISSN: 0018-9200

Agilent Application Note (2000). Characterizing Digitally Modulated Signals with CCDF Curves, No. 5968-6875E, Agilent Technologies, Inc., Santa Clara, USA

Akos, D.; Stockmaster, M.; Tsui, J. & Caschera, J. (1999). Direct Bandpass Sampling of Multiple Distinct RF Signals, *IEEE Transactions on Communications*, Vol. 47, No. 7, July 1999, pp. 983-988

Bauml, R.; Fischer, R. & Huber, J. (1996). Reducing the peak-to-average power ratio of multicarrier modulation by selected mapping, *Electronic Letters*, 1996, Vol. 32, pp. 2056-2057

Besser, L. & Gilmore, R. (2003). *Practical RF Circuit Design for Modern Wireless Systems,* Artech House, ISBN 1-58053-521-6, Norwood, USA

Cruz, P.; Carvalho, N.B. & Remley, K.A. (2008), Evaluation of Nonlinear Distortion in ADCs Using Multisines, *IEEE MTT-S International Microwave Symposium Digest*, pp. 1433-1436, ISBN: 978-1-4244-1780-3, Atlanta, USA, June 2008

Cruz, P.; Carvalho, N.B.; Remley, K.A. & Gard, K.G. (2008). Mixed Analog-Digital Instrumentation for Software Defined Radio Characterization, *IEEE MTT-S International Microwave Symposium Digest*, pp. 253-256, ISBN: 978-1-4244-1780-3, Atlanta, USA, June 2008

Cruz, P. & Carvalho, N.B. (2008). PAPR Evaluation in Multi-Mode SDR Transceivers, *38th European Microwave Conference*, pp. 1354-1357, ISBN: 978-2-87487-006-4, Amsterdam, Netherlands, October 2008

Goldsmith, A. & Chua, S. (1998). Adaptive Coded Modulation for Fading Channels, *IEEE Transactions on Communications*, Vol.46, No. 5, May 1998, pp. 595-602, ISSN: 0090-6778

Gomes, H.; Carvalho, N.B. (2007). The use of Intermodulation Distortion for the Design of Passive RFID, *37th European Microwave Conference*, pp. 1656-1659, ISBN: 978-2-87487-001-9, Munich, Germany, October 2007

Gomes, H.; Carvalho, N.B. (2009). RFID for Location Proposes Based on the Intermodulation Distortion, *Sensors & Transducers journal*, Vol. 106, No. 7, pp. 85-96, July 2009, ISSN 1726-5479

Han, S.H. & Lee, J.H. (2003). Reduction of PAPR of an OFDM Signal by Partial Transmit Sequence Technique with Reduced Complexity, *IEEE Global Telecommunications Conference*, pp. 1326-1329, ISBN: 0-7803-7974-8, San Franscisco, USA, December 2003

Han, S.H. & Lee, J.H. (2005). An Overview of Peak-to-Average Power Ratio Reduction Techniques for Multicarrier Transmission, *IEEE Wireless Communications*, Vol. 12, No. 2, pp. 56-65, April 2005

Han, S.H.; Cioffi, J.M. & Lee, J.H. (2006). Tone Injection with Hexagonal Constellation for Peak-to-Average Power Ratio Reduction in OFDM, *IEEE Communications Letters*, Vol. 10, No. 9, pp. 646-648, September 2006, ISSN: 1089-7798

IEEE 802.16e standard (2005). Local and Metropolitan Networks – Part 16: Air Interface for Fixed and Mobile Broadband Wireless Access Systems, 2005

Jiang, T.; Yang, Y. & Song, Y. (2005). Exponential Companding Technique for PAPR Reduction in OFDM Systems, *IEEE Transactions on Broadcasting*, Vol. 51, No. 2, pp. 244-248, June 2005, ISSN: 0018-9316

Krongold, B.S. & Jones, D.L. (2003). PAR Reduction in OFDM via Active Constellation Extension, *IEEE Transactions on Broadcasting*, Vol. 49, No. 3, pp. 258-268, September 2003, ISSN: 0018-9316

Landon, V.D. (1936). A Study of the Characteristics of Noise, *Proceedings of the IRE*, Vol. 24, No. 11, pp. 1514-1521, November 1936, ISSN: 0096-8390

Muhammad, K.; Ho, Y.C.; Mayhugh, T.; Hung, C.M.; Jung, T.; Elahi, I.; Lin, C.; Deng, I.; Fernando, C.; Wallberg, J.; Vemulapalli, S.; Larson, S.; Murphy, T.; Leipold, D.; Cruise, P.; Jaehnig, J.; Lee, M.C.; Staszewski, R.B.; Staszewski, R.; Maggio, K. (2005). A Discrete Time Quad-Band GSM/GPRS Receiver in a 90nm Digital CMOS Process, *Proceedings of IEEE 2005 Custom Integrated Circuits Conference*, pp. 809-812, ISBN 0-7803-9023-7, San Jose, USA, September 2005

Park, J.; Lee, C.; Kim, B. & Laskar, J. (2006). Design and Analysis of Low Flicker-Noise CMOS Mixers for Direct-Conversion Receivers, *IEEE Transactions on Microwave Theory and Techniques*, Vol. 54, No. 12, December 2006, pp. 4372-4380, ISSN: 0018-9480

Pedro, J.C. & Carvalho, N.B. (2003). *Intermodulation Distortion in Microwave and Wireless Circuits*, Artech House, ISBN 1-58053-356-6, Norwood, USA

Pedro, J.C. & Carvalho, N.B. (2005). Designing Multisine Excitations for Nonlinear Model Testing, *IEEE Transactions Microwave Theory and Techniques,* Vol. 53, No. 1, pp. 45-54, January 2005, ISSN: 0018-9480

Razavi, B. (1997). Design Considerations for Direct–Conversion Receivers. *IEEE Transactions on Circuits and Systems – II: Analog and Digital Signal Processing*, Vol. 44, No. 6, June 1997, pp. 428-435, ISSN 1057-7130

Razavi, B. (1998). Architectures and Circuits for RF CMOS Receivers, *Proceedings of IEEE 1998 Custom Integrated Circuits Conference*, pp. 393-400, ISBN 0-7803-4292-5, Santa Clara, USA, May 1998

Remley, K.A. (2003). Multisine Excitation for ACPR Measurements, *IEEE MTT-S International Microwave Symposium Digest*, pp. 2141-2144, ISBN: 0-7803-7695-1, Philadelphia, USA, June 2003

Staszewski, R.B.; Muhammad, K.; Leipold, D.; Chih-Ming Hung; Yo-Chuol Ho; Wallberg, J.L.; Fernando, C.; Maggio, K.; Staszewski, R.; Jung, T.; Jinseok Koh; John, S.; Irene Yuanying Deng; Sarda, V.; Moreira-Tamayo, O.; Mayega, V.; Katz, R.; Friedman, O.; Eliezer, O.E.; de-Obaldia, E.; Balsara, P.T. (2004). All-Digital TX Frequency Synthesizer and Discrete-Time Receiver for Bluetooth Radio in 130-nm CMOS, *IEEE Journal of Solid-State Circuits*, Vol. 39, No. 12, December 2004, pp. 2278-2291, ISSN: 0018-9200

Tellado, J. & Cioffi, J.M. (1998). Peak Power Reduction for Multicarrier Transmission, *IEEE Global Telecommunications Conference*, Sydney, Australia, Nov. 1998.

Tsui, J. (1995). *Digital Techniques for Wideband Receivers,* Artech House, ISBN 0-89006-808-9, Norwood, USA

Vaananen, O.; Vankka, J. & Halonen, K. (2002). Reducing the Peak-to-Average Ratio of Multicarrier GSM and EDGE Signals, *IEEE International Symposium on Personal, Indoor and Mobile Radio Communications*, pp. 115-119, ISBN: 0-7803-7589-0, Lisbon, Portugal, September 2002

Vaughan, R.; Scott, N. & White, D. (1991). The Theory of Bandpass Sampling, *IEEE Transactions on Signal Processing*, Vol. 39, No. 9, September 1991, pp. 1973-1984, ISSN: 0090-6778

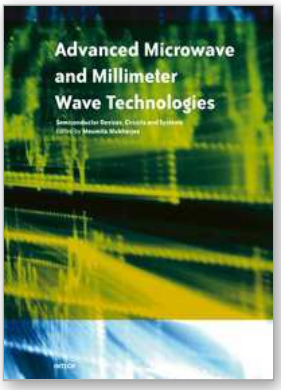

Advanced Microwave and Millimeter Wave Technologies
Semiconductor Devices Circuits and Systems
Edited by Moumita Mukherjee

ISBN 978-953-307-031-5
Hard cover, 642 pages
Publisher InTech
Published online 01, March, 2010
Published in print edition March, 2010

This book is planned to publish with an objective to provide a state-of-the-art reference book in the areas of advanced microwave, MM-Wave and THz devices, antennas and systemtechnologies for microwave communication engineers, Scientists and post-graduate students of electrical and electronics engineering, applied physicists. This reference book is a collection of 30 Chapters characterized in 3 parts: Advanced Microwave and MM-wave devices, integrated microwave and MM-wave circuits and Antennas and advanced microwave computer techniques, focusing on simulation, theories and applications. This book provides a comprehensive overview of the components and devices used in microwave and MM-Wave circuits, including microwave transmission lines, resonators, filters, ferrite devices, solid state devices, transistor oscillators and amplifiers, directional couplers, microstripeline components, microwave detectors, mixers, converters and harmonic generators, and microwave solid-state switches, phase shifters and attenuators. Several applications area also discusses here, like consumer, industrial, biomedical, and chemical applications of microwave technology. It also covers microwave instrumentation and measurement, thermodynamics, and applications in navigation and radio communication.

How to reference
In order to correctly reference this scholarly work, feel free to copy and paste the following:

Pedro Cruz, Hugo Gomes and Nuno Carvalho (2010). Receiver Front-End Architectures – Analysis and Evaluation, Advanced Microwave and Millimeter Wave Technologies Semiconductor Devices Circuits and Systems, Moumita Mukherjee (Ed.), ISBN: 978-953-307-031-5, InTech, Available from: http://www.intechopen.com/books/advanced-microwave-and-millimeter-wave-technologies-semiconductor-devices-circuits-and-systems/receiver-front-end-architectures-analysis-and-evaluation

INTECH
open science | open minds

InTech Europe
University Campus STeP Ri
Slavka Krautzeka 83/A
51000 Rijeka, Croatia
Phone: +385 (51) 770 447
Fax: +385 (51) 686 166
www.intechopen.com

InTech China
Unit 405, Office Block, Hotel Equatorial Shanghai
No.65, Yan An Road (West), Shanghai, 200040, China
中国上海市延安西路65号上海国际贵都大饭店办公楼405单元
Phone: +86-21-62489820
Fax: +86-21-62489821